

# Kondo screening of Andreev bound states in an N-QD-S system

Lin Li,<sup>1</sup> Zhan Cao,<sup>2</sup> Tie-Feng Fang,<sup>2</sup> Hong-Gang Luo,<sup>2,3</sup> and Wei-Qiang Chen<sup>1</sup>

<sup>1</sup>*Department of physics, Southern University of science and technology of China, Shenzhen 518005, China*

<sup>2</sup>*Center of Interdisciplinary Studies and Key Laboratory for Magnetism and Magnetic Materials of the Ministry of Education, Lanzhou University, Lanzhou 730000, China*

<sup>3</sup>*Beijing Computational Science Research Center, Beijing 100084, China*

Motivated by experimental observation of the Kondo-enhanced Andreev transport [R. S. Deacon *et al.*, PRB **81**, 121308(R) (2010)] in a hybrid normal metal-quantum dot-superconductor (N-QD-S) device, we theoretically study the Kondo effect in such a device and clarify the different roles played by the normal and superconducting leads. Due to the Andreev reflection in a QD-S system, a pair of Andreev energy levels form in the superconducting gap, which is able to carry the magnetic moment if the ground state of the QD is a magnetic doublet. In this sense, the Andreev energy levels play a role of effective impurity levels. When the normal lead is coupled to the QD-S system, on the one hand, the Andreev energy levels broaden to form the so-called Andreev bound states (ABSs), on the other hand, it can screen the magnetic moment of the ABSs. By tuning the couplings between the QD and the normal (superconducting) leads, the ABSs can simulate the Kondo, mixed-valence, and even empty orbit regimes of the usual single-impurity Anderson model. The above picture is confirmed by the Green's function calculation of the hybrid N-QD-S Anderson model and is also able to explain qualitatively experimental phenomena observed by Deacon *et al.*. These results can further stimulate related experimental study in the N-QD-S systems.

## I. INTRODUCTION

The Kondo physics resulted from the screening of the local moment by conduction electrons<sup>1</sup> provides an ideal platform to explore the many-body correlations and their interactions. Below certain temperature (the Kondo temperature  $T_K$ ) the Kondo physics is characterized by a resonance developed near the Fermi energy level. When the conduction electrons consist of a conventional superconducting quasi-particles described by a gapped excitation spectrum, the interplay between the magnetism and superconductivity creates the so called Yu-Shiba-Rusinov (YSR) bound state.<sup>2-5</sup> On the other hand, the competition between the Kondo and superconducting correlation also determines the ground state of such systems. It is a magnetic doublet if the superconducting correlation dominates over the Kondo effect, otherwise, the ground state is a spin singlet state.<sup>6</sup>

In a junction consisting of metal and superconductor, the transport shows a unique feature, namely, the Andreev reflection. When a low-energy electron is incident on the interface, a Cooper pair is injected into the superconductor and as a result, a hole with opposite spin is generated to go back into the metal. In a confined geometry, this process is able to create a pair of discrete Andreev energy levels [see Fig. 1 (a)] in the superconducting gap, as proposed theoretically.<sup>7-13</sup> When a normal metal electrode is additionally coupled to the system [see Fig. 1 (b)], the discrete Andreev energy levels can broaden to form the so-called Andreev bound states (ABSs). Recently, the individual ABSs have been clearly identified in a semiconductor quantum dot (QD) connected with normal and superconducting leads (N-QD-S)<sup>14-16</sup> and in a superconductor-QD hybrid with graphene.<sup>17</sup> In a successive paper,<sup>18</sup> Deacon *et al.* further found that a Kondo resonance occurs around the Fermi level if the

coupling between the QD and the normal lead ( $\Gamma_N$ ) is much smaller than the coupling between the QD and the superconducting lead ( $\Gamma_S$ ), as shown schematically in Fig.1 (c). However, in the opposite case, namely,  $\Gamma_N \gg \Gamma_S$ , the Kondo resonance near the Fermi level has not been observed. Furthermore, once the superconducting gap is killed by applied magnetic field, the Kondo peaks with Zeeman splitting have been observed. Though there do exist many theoretical works to investigate the Kondo effect in the N-QD-S device,<sup>19-27</sup> some fundamental issues involved in the Deacon *et al.*'s experiment can not be clearly explained. For example, if the superconducting lead is available, one can not observe the Kondo resonance if  $\Gamma_N \gg \Gamma_S$  and oppositely, the Kondo resonance occurs if  $\Gamma_S \gg \Gamma_N$ . When the superconductivity is killed by applied magnetic field, the Kondo resonances with Zeeman splitting have been observed in both cases. What is the underlying physics? More fundamentally, what is the role played by the superconducting lead in such a hybrid N-QD-S device?

In this work, we make an attempt to understand these experimental observations. Fig.1 (d)-(f) represent our physical picture, which shows schematically the microscopic mechanism of the Kondo resonance observed in the experiment.<sup>18</sup> The key point of this picture is that the coupling between the QD and the superconducting lead induces a pair of Andreev bound levels, which are able to carry effective magnetic moment [denoted by blue dashed arrow in Fig. 1 (d)-(f)] originated from the single occupancy of the dot level if the ground state of the QD is a magnetic doublet. In the spin-flip cotunneling process of the QD, equivalently, the effective magnetic moment involved in the ABSs is reversed. In this sense, the effective magnetic moment of the ABSs is screened by the conduction electrons in the normal lead, which leads to the Kondo resonance observed in the experiment.<sup>18</sup>

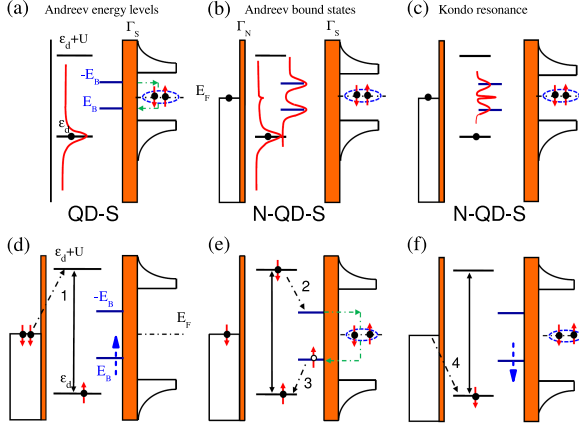


FIG. 1. (a)-(c) The schematic ABSs and Kondo resonance in the N-QD-S device. (a) In the absence of the normal lead ( $\Gamma_N = 0$ ), the ABSs manifest as discrete Andreev energy levels located at  $\pm E_B$ . (b) Once the normal lead is switched on ( $\Gamma_N \neq 0$ ), the discrete Andreev energy levels broaden to form the ABSs with the width in the order of  $\Gamma_N$ . (c) The Kondo resonance occurs once the temperature decreases to certain characteristic temperature  $T_K$ . (d)-(f) The schematic picture of the Kondo resonance lead by an effective spin-flip cotunneling process marked by 1 to 4. (d) The initial state: a spin-up electron on the dot level  $\varepsilon_d$  forms a magnetic moment due to large  $U$ . The strong coupling with the superconducting lead induces the ABSs, which are able to carry this magnetic moment, as shown as blue dashed arrow. “1” denotes the virtual process of double occupancy of the dot. (e) The intermediate states: by the process of “2”, a Cooper pair forms in the superconducting lead and the spin-up electron combines with a hole generated by Andreev reflection, denoted by the process “3”. (f) The final state: one spin-down electron tunnels into the dot level denoted by the process “4”, equivalently, the spin in the dot level is reversed. Meanwhile, the effective magnetic moment in the ABSs is also reversed effectively. As a result, the effective magnetic moment in the ABSs has been screened by the electrons in the normal lead, which leads to the Kondo resonance in the N-QD-S device.

Differently from the Kondo effect in the usual normal metal-quantum dot-normal metal (N-QD-N) device, the spin-flip cotunneling process here is associated with the Andreev reflection process, in which the effective magnetic moment determined by the position of the ABSs plays an important role in such a device. Therefore, one can imagine that the position of the ABSs can be tuned by changing various parameters of the N-QD-S device, as a result, this device can simulate various regimes involved in the single-impurity Anderson model (SIAM),<sup>28</sup> for example, the Kondo regime, the mixed-valence regime, and even the empty orbit regime, as discussed in detail later. Our results can explain qualitatively the experimental observations and thus clarify the questions mentioned above.

## II. MODEL AND FORMALISM

To confirm above physical picture, in the following we consider the N-QD-S device described by a hybrid Anderson impurity model. The Hamiltonian reads

$$H = \sum_{\beta=N,S} H_{\beta} + H_d + H_V, \quad (1)$$

where  $H_d = \sum_{\sigma} \varepsilon_{d\sigma} d_{\sigma}^{\dagger} d_{\sigma} + U n_{d\uparrow} n_{d\downarrow}$  describes the QD with the energy level  $\varepsilon_{d\sigma}$  and the on-site repulsion interaction  $U$ .  $H_{\beta} = \sum_{k\sigma} \varepsilon_{k\beta} c_{k\sigma\beta}^{\dagger} c_{k\sigma\beta} + \delta_{\beta,S} \Delta \sum_k (c_{k\uparrow\beta}^{\dagger} c_{-k\downarrow\beta}^{\dagger} + H.c.)$  is the Hamiltonian of the normal ( $\beta = N$ ) and the superconducting ( $\beta = S$ ) leads, which are contacted to the QD by the coupling term  $H_V = \sum_{k\sigma\beta} (V_{k\beta} c_{k\sigma\beta}^{\dagger} d_{\sigma} + H.c.)$ . Here  $\Delta$  is superconducting gap and  $V_{k\beta}$  is the coupling strength with the  $\beta$ -lead.

Due to the superconducting proximity effect, it is convenient to express the retarded dot Green's function (GF) by using the Nambu representation, namely,  $\hat{G}_{d\sigma}(t, t') = \langle\langle \hat{\Psi}_{\sigma}(t); \hat{\Psi}_{\sigma}^{\dagger}(t') \rangle\rangle$  with  $\hat{\Psi}_{\sigma}^{\dagger} = (d_{\sigma}^{\dagger}, d_{\bar{\sigma}})$  and  $\hat{\Psi}_{\sigma} = (\hat{\Psi}_{\sigma}^{\dagger})^{\dagger}$ . In the frequency space, the GF has a form of Dyson equation

$$[\hat{G}_{d\sigma}(\omega)]^{-1} = [\hat{G}_{d\sigma}^0(\omega)]^{-1} - \hat{\Sigma}_{\sigma}^U(\omega), \quad (2)$$

where  $[\hat{G}_{d\sigma}^0(\omega)]^{-1} = \hat{I}\omega - \hat{\sigma}_z \text{diag}(\varepsilon_{d\sigma}, \varepsilon_{d\bar{\sigma}}) - \hat{\Sigma}^0(\omega)$ . Here  $\hat{\Sigma}^0(\omega)$  is the non-interacting self-energy with the components  $\hat{\Sigma}_{11}^0(\omega) = \hat{\Sigma}_{22}^0(\omega) = -i(\Gamma_N + \Gamma_S \rho_S(\omega)) = -i\Gamma(\omega)$ ,  $\hat{\Sigma}_{12}^0(\omega) = \hat{\Sigma}_{21}^0(\omega) = i\frac{\sigma\Delta}{\omega} \Gamma_S \rho_S(\omega)$ ,  $\rho_S(\omega) = \frac{|\omega| \theta(|\omega| - \Delta)}{\sqrt{\omega^2 - \Delta^2}} + \frac{\omega \theta(\Delta - \omega)}{i\sqrt{\Delta^2 - \omega^2}}$ , and the coupling  $\Gamma_{\beta} = \pi |V_{k\beta}|^2 / (2D)$ .<sup>29,30</sup> Here we take the coupling matrix element  $V_{k\beta}$  to be  $k$ -independent and shall restrict to the limit  $|\varepsilon_{k\beta}| \ll D$ , where  $D$  is the half-bandwidth. The self-energy  $\hat{\Sigma}_{\sigma}^U(\omega)$  is due to the on-site repulsion interaction, denoting correlation effect.<sup>31-33</sup> Following the notations introduced in Refs. [34] and [35], the self-energy  $\hat{\Sigma}_{\sigma}^U(\omega)$  has a matrix form  $\hat{\Sigma}_{\sigma}^U(\omega) = U \hat{F}_{d\sigma}(\omega) [\hat{G}_{d\sigma}(\omega)]^{-1}$ , where

$$\hat{F}_{d\sigma}(\omega) = \begin{pmatrix} \langle\langle d_{\sigma} n_{d\bar{\sigma}}; d_{\sigma}^{\dagger} \rangle\rangle & \langle\langle d_{\sigma} n_{d\bar{\sigma}}; d_{\bar{\sigma}} \rangle\rangle \\ -\langle\langle d_{\bar{\sigma}}^{\dagger} n_{d\sigma}; d_{\sigma}^{\dagger} \rangle\rangle & -\langle\langle d_{\bar{\sigma}}^{\dagger} n_{d\sigma}; d_{\bar{\sigma}} \rangle\rangle \end{pmatrix}. \quad (3)$$

In the framework of equation of motion of GF, this self-energy cannot be obtained exactly, and one has to employ truncation approximation. As shown by Eq.(25) in Appendix, the high-order GFs in Eq. (26) can be treated conventionally by a cluster expansion,<sup>36</sup> where the connected GFs like  $\langle\langle d_{\sigma} n_{d\bar{\sigma}}; d_{\sigma}^{\dagger} \rangle\rangle_c$  contains the contribution from the more higher order correlation effect, which can be truncated at different approximate level. As truncated in the first order, the Hartree-Fock approximation (HFA) can be reached by neglecting the connected GFs  $\hat{F}_{d\sigma}(\omega)_c$  as defined in Appendix. In this case the self-

energy  $\hat{\Sigma}_\sigma^U(\omega)$  is approximated by

$$\hat{\Sigma}_\sigma^U(\omega) \approx \hat{\Sigma}_\sigma^{HF}(\omega) = U \begin{pmatrix} \langle n_{d\bar{\sigma}} \rangle & \langle d_{\bar{\sigma}} d_\sigma \rangle \\ \langle d_\sigma^\dagger d_{\bar{\sigma}}^\dagger \rangle & -\langle n_{d\sigma} \rangle \end{pmatrix}, \quad (4)$$

where the occupation  $\langle n_{d\bar{\sigma}} \rangle = -\frac{1}{\pi} \int f(\omega) \text{Im}[\hat{G}_{d\bar{\sigma}}(\omega)]_{11} d\omega$ ,  $f(\omega)$  is the Fermi distribution function.<sup>25,33,37</sup>  $\langle d_\sigma^\dagger d_{\bar{\sigma}}^\dagger \rangle$  is the pairing correlation function of the QD, which can be explicitly evaluated with  $\langle d_\sigma^\dagger d_{\bar{\sigma}}^\dagger \rangle = -\frac{1}{\pi} \int f(\omega) \text{Im}[\hat{G}_{d\sigma}(\omega)]_{21} d\omega$ , where the anomalous GF obtained is

$$\left[ \hat{G}_{d\sigma}(\omega) \right]_{21} = \frac{\hat{\Sigma}_{21}^0(\omega) + U \langle d_\sigma^\dagger d_{\bar{\sigma}}^\dagger \rangle}{\omega + \varepsilon_{d\bar{\sigma}} + i\Gamma(\omega) + U \langle n_{d\sigma} \rangle} \left[ \hat{G}_{d\sigma}(\omega) \right]_{11}. \quad (5)$$

[see Eq.(28) in Appendix] The HFA has been used to treat the level-crossing quantum phase transition between the BCS-singlet and the magnetic doublet states,<sup>16,33,38,39</sup> and it is also useful to determine the magnetic regime of the N-QD-S device as following the

scheme of Anderson.<sup>28</sup> However, it is well-known that in the HFA level the Kondo effect is absent, and thus one needs to consider the high-order GF's (see, e.g., Refs.[36] and [40]).

To capture the Kondo physics, one only needs to consider the contribution of diagonal connected GFs, such as  $\langle \langle d_\sigma n_{d\bar{\sigma}}; d_\sigma^\dagger \rangle \rangle_c$ ,<sup>31,32,41</sup> because the non-diagonal components like  $\langle \langle d_{\bar{\sigma}}^\dagger n_{d\sigma}; d_\sigma^\dagger \rangle \rangle_c$  will introduce additional influence of the correlation effect on the superconducting lead, in which we are not interested. Here we take the Lacroix's truncation approximation,<sup>40</sup> as widely used in the literature.<sup>42-48</sup> For details, one can refer to Appendix. Under this approximation, the "11"-component of the dot GF reads

$$\left[ \hat{G}_{d\sigma}(\omega) \right]_{11} = \frac{1}{R_\sigma(\omega) - U[Q_\sigma(\omega) + T_\sigma(\omega)]/P_\sigma(\omega)}, \quad (6)$$

where the following notations have been introduced for clarity,

$$R_\sigma(\omega) = \omega - \varepsilon_{d\sigma} + i\Gamma(\omega) - U \langle n_{d\bar{\sigma}} \rangle - \frac{(\hat{\Sigma}_{21}^0(\omega) + U \langle d_{\bar{\sigma}} d_\sigma \rangle)(\hat{\Sigma}_{21}^0(\omega) + U \langle d_\sigma^\dagger d_{\bar{\sigma}}^\dagger \rangle)}{\omega + \varepsilon_{d\bar{\sigma}} + i\Gamma(\omega) + U \langle n_{d\sigma} \rangle}, \quad (7)$$

$$P_\sigma(\omega) = \omega - \varepsilon_{d\sigma} - U(1 - \langle n_{d\bar{\sigma}} \rangle) + 3i\Gamma(\omega) + U(A_{1\sigma}(\omega) - A_{2\sigma}(\omega)), \quad (8)$$

$$Q_\sigma(\omega) = (\omega - \varepsilon_{d\sigma} - U \langle n_{d\bar{\sigma}} \rangle)(A_{1\sigma}(\omega) - A_{2\sigma}(\omega)) + U[\langle n_{d\bar{\sigma}} \rangle(1 - \langle n_{d\bar{\sigma}} \rangle) - \langle d_{\bar{\sigma}} d_\sigma \rangle \langle d_\sigma^\dagger d_{\bar{\sigma}}^\dagger \rangle] - 2i\Gamma(\omega) \langle n_{d\bar{\sigma}} \rangle - (B_{1\sigma}(\omega) + B_{2\sigma}(\omega)), \quad (9)$$

$$T_\sigma(\omega) = [\varepsilon_{d\sigma} + \varepsilon_{d\bar{\sigma}} + U(1 + \langle n_{d\sigma} \rangle - \langle n_{d\bar{\sigma}} \rangle)] \frac{\langle d_{\bar{\sigma}} d_\sigma \rangle (\hat{\Sigma}_{21}^0(\omega) + U \langle d_\sigma^\dagger d_{\bar{\sigma}}^\dagger \rangle)}{\omega + \varepsilon_{d\bar{\sigma}} + i\Gamma(\omega) + U \langle n_{d\sigma} \rangle}, \quad (10)$$

with

$$A_{i\sigma}(\omega) = \frac{i}{2\pi^2} \sum_{\beta=(N,S)} \int \int d\omega' d\varepsilon \Gamma_\beta f(\omega') \frac{\frac{(z'_+ + \varepsilon)[\hat{G}_{d\bar{\sigma}}(\omega')]_{11} - \delta_{\beta,S} \bar{\sigma} \Delta [\hat{G}_{d\bar{\sigma}}(\omega')]_{21} - (z'_+ + \varepsilon)[\hat{G}_{d\bar{\sigma}}(\omega')]_{11}^* - \delta_{\beta,S} \bar{\sigma} \Delta [\hat{G}_{d\bar{\sigma}}(\omega')]_{21}^*}{(z'_+ - \varepsilon)(z'_+ + \varepsilon) - \delta_{\beta,S} \Delta^2}}{z_+ - \varepsilon_{i\sigma}}, \quad (11)$$

and

$$B_{i\sigma}(\omega) \approx \frac{1}{\pi} \int d\varepsilon \frac{\Gamma_N f(\varepsilon) [1 - i\Gamma_N (\hat{G}_{d\bar{\sigma}}(\varepsilon))_{11}]}{z_+ - \varepsilon_{i\sigma}} + \frac{i}{2\pi^2} \int \int d\omega' d\varepsilon \Gamma_S(\varepsilon) f(\omega') \frac{\frac{z'_+ + \varepsilon}{(z'_+ - \varepsilon)(z'_+ + \varepsilon) - \Delta^2} - \frac{z'_- + \varepsilon}{(z'_- - \varepsilon)(z'_- + \varepsilon) - \Delta^2}}{z_+ - \varepsilon_{i\sigma}}, \quad (12)$$

where  $z_\pm = \omega \pm i\eta$  ( $\eta \rightarrow 0^+$ ), and  $\varepsilon_{1\sigma} = \varepsilon + \varepsilon_{d\sigma} - \varepsilon_{d\bar{\sigma}}$ ,  $\varepsilon_{2\sigma} = -\varepsilon + \varepsilon_{d\bar{\sigma}} + \varepsilon_{d\sigma} + U$ . The GF's in Eqs.(5) and (6) are closed and can be calculated self-consistently. The equation of motion treatment is simple enough, but it is quite good at high temperature, and it can capture qualitatively the Kondo physics even at low temperatures. The main goal of the present work is to explain not quantitatively but qualitatively the experimental observations given by Deacon *et al.*,<sup>18</sup> and thus the result of the equation of motion is sufficient to confirm our physical picture.

### III. NUMERICAL RESULTS

In order to obtain the Kondo resonance, we discuss the local density of states  $\rho_d(\omega) = -\frac{1}{\pi} \sum_\sigma \text{Im}[\hat{G}_{d\sigma}(\omega)]_{11}$  of the QD. In our calculations, the superconducting gap  $\Delta$  is taken as the units of energy, and the half bandwidth  $D = 20\Delta$ .

To extract the role of normal and superconducting leads in the Kondo screening, we show the development and evolution of Kondo resonance by tuning the coupling  $\Gamma_N$  and  $\Gamma_S$  in Fig.2 (a) and (b), respectively. The position of ABSs level  $E_B$ , corresponding to the pair breaking

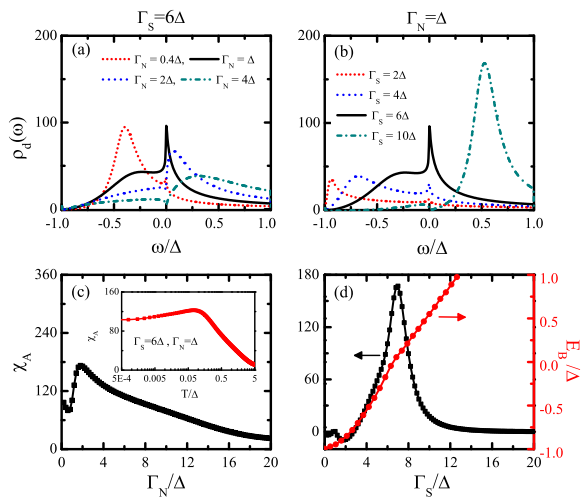


FIG. 2. (a)-(b) The evolution of Kondo resonance and ABS in the local density of states by tuning the couplings of  $\Gamma_N$  and  $\Gamma_S$ , respectively. (c)-(d) The spin susceptibility of the ABS as a function of the couplings of  $\Gamma_N$  and  $\Gamma_S$ .  $\Gamma_S = 6\Delta$  in (a) and (c) and  $\Gamma_N = \Delta$  in (b) and (d). The red dotted-line in (d) indicates the coupling ( $\Gamma_S$ ) dependent of the Andreev bound level  $E_B$ . Other parameters used are the dot level  $\varepsilon_{d\sigma} = -5\Delta$ , the Coulomb interaction  $U = 40\Delta$ , and the temperature  $T = 0$ . The inset of (c) is the temperature dependent susceptibility.

excitation due to the local spin, is mainly determined by the coupling  $\Gamma_S$ . When the level  $E_B$  is situated below the Fermi level, the ground state of QD is a magnetic doublet state.<sup>6,48,49</sup> Once the normal lead is applied, the ABSs are broadened and at the same time, a Kondo resonance at the Fermi level is developed, as shown in Fig.2 (a). For fixed  $\Gamma_S = 6\Delta$ , the Kondo resonance evolves from a peak ( $\Gamma_N = 0.4\Delta, \Delta$ ) into an asymmetric structure ( $\Gamma_N = 2\Delta, 4\Delta$ ) by increasing the coupling  $\Gamma_N$ . The asymmetric structures originate from the Fano resonance created by the interference of Kondo resonance and significant broadened ABSs.<sup>50</sup> These are the typical behaviors of the SIAM ranging from the Kondo to mixed-valence regime.<sup>51,52</sup> The above results indicate that the ABSs can be recognized as a localized level with an effective moment. Physically, the moment of ABSs originates from the quasi-particle excited by the pair-broken scattering of local spin. The level  $E_B$  can be broadened and screened by applied normal lead, accordingly, creating a significant pronounced Kondo resonance peak at the Fermi level. In Fig. 1, we showed the microscopic mechanism of Kondo screening in the N-QD-S device, where the screening of the local spin in the QD can be equivalently seen as a process that the effective moment of ABSs is screened through the associated Andreev reflection.

In order to clarify the magnetic nature of the ABSs and its screening process, in Fig.2 (c), we show the spin susceptibility of the ABS defined by  $\chi_A = \frac{g\mu_B(n_{A\uparrow} - n_{A\downarrow})}{h}|_{h \rightarrow 0}$ , where  $n_{A\sigma} =$

$-\frac{1}{\pi} \int_{-\Delta}^{+\Delta} f(\omega) \text{Im}[\hat{G}_{d\sigma}(\omega)]_{11} d\omega$  is the occupation of ABS existing in the superconducting gap. In addition,  $h$  is a weak applied magnetic field,  $g$  is the Landé factor,  $\mu_B$  is the Bohr magneton, and we take  $g\mu_B = 1$ . **It is seen that the susceptibility can be suppressed by increasing  $\Gamma_N$ , which indicates the Kondo screening of the effective moment of ABS by the conduction electrons in normal lead. While the increasing in the susceptibility with  $\Gamma_N \lesssim 2\Delta$  may correspond to the enhancement of local moment in the ABS.** In addition, the inset of Fig. 2 (c) shows the temperature dependence of susceptibility  $\chi_A$ , which is qualitatively consistent with the general Kondo screening behavior of local moment.<sup>53</sup> Therefore, the Kondo effect in the N-QD-S can be simply described by the Kondo screening of the ABSs.

It is well-known that changing the Anderson impurity system from the Kondo regime, to the mixed-valence regime, and even to the empty orbit regime can be realized by tuning the impurity level. Here we fix  $\Gamma_N = \Delta$  and tune the level position of  $E_B$  by increasing  $\Gamma_S$  from  $2\Delta$  to  $10\Delta$ , as shown in Fig.2 (b). It is seen that the Kondo resonance takes place when the ground state of QD is a magnetic doublet state ( $\Gamma_S = 2\Delta, 4\Delta, 6\Delta$ ). In contrast, the Kondo resonance disappears as the ABSs shift above Fermi level (in empty orbit regime), because the ground state is a Kondo singlet state ( $\Gamma_S = 10\Delta$ ) even without the normal lead. Likewise, we calculate  $\chi_A$  as a function of  $\Gamma_S$ , as shown in Fig.2 (d) for the squared-line. With increasing  $\Gamma_S$ ,  $\chi_A$  increases firstly, and then decreases dramatically. The former can be understood as follows. When  $\Gamma_S$  is switched on, the ABSs begins to form at the gap edge but with small weight, and the effective local moment of ABSs gradually develops (the negative  $\chi_A$  for some small  $\Gamma_S$  may be artificial of the truncation approximation). With increasing  $\Gamma_S$ , the ABSs begin to move toward the Fermi level, as shown in Fig. 2 (d) for dotted-line curve, and its weight and as a result the effective magnetic moment, also increases. At the same time, the effective magnetic moment would be screened by the conduction electrons in the normal metal, leading to the Kondo resonance peak around the Fermi level, as shown in Figs. 2(a,b). Once the ABSs crosses the Fermi level, it seems that the system enters into a mixed valence or an empty orbit regime,  $\chi_A$  decreases rapidly up to zero. In this sense, the coupling  $\Gamma_S$  in the N-QD-S device just plays a role of gate-voltage in the usual N-QD-N device.

To confirm the above picture, we consider the Andreev transport in the N-QD-S device. The Andreev conductance is  $G_A = \frac{dI_A}{dV_{sd}}$  with  $I_A = \frac{2e}{h} \int \Gamma_N^2 |[\hat{G}_{d\sigma}(\omega)]_{21}|^2 [f_N(\varepsilon - eV_{sd}) - f_N(\varepsilon + eV_{sd})] d\varepsilon$ , as measured in the Deacon *et al.*'s experiment.<sup>18</sup> Fig. 3 (a) and (b) show the results for the cases  $\Gamma_S \gg \Gamma_N$  and  $\Gamma_N \gg \Gamma_S$ , respectively. For the former one there exists three peaks, and the central one is the Kondo resonance, which is qualitatively consistent with the experimental observation. For the latter one the Kondo res-

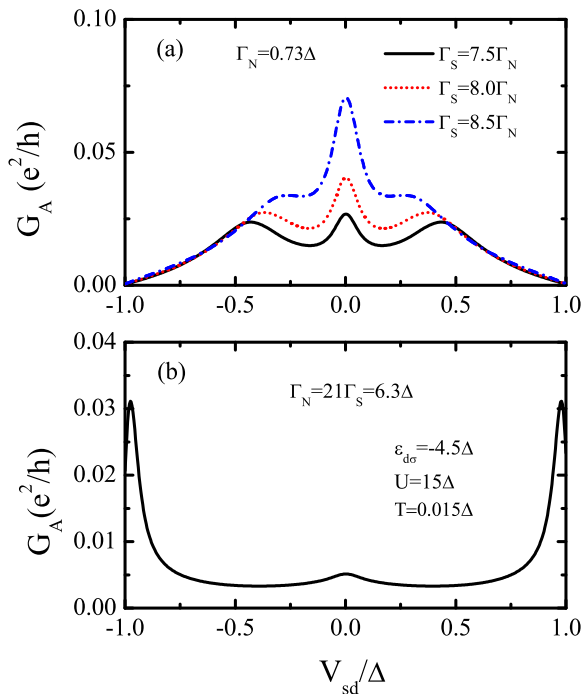


FIG. 3. The Andreev transport of the N-QD-S device for (a)  $\Gamma_S = (7.5, 8.0, 8.5)\Gamma_N$  and (b)  $\Gamma_N = 21\Gamma_S$ . Other parameters used are also similar to those in the Deacon *et al.*'s experiment<sup>18</sup> with the dot level  $\varepsilon_{d\sigma} = -4.5\Delta$ , the temperature  $T = 0.015\Delta$ , and the Coulomb interaction  $U = 15\Delta$ .

onance is strongly suppressed and the ABSs are located around the edge of the superconducting gap, which is also similar to that observed in the experiment. Our results give a physically reasonable explanation of the Deacon *et al.*'s experiment.<sup>18</sup> The underlying physical mechanism is the Kondo screening of the ABSs, which shows the constructive effect of the superconducting lead on the Kondo transport. In order to further confirm this, we compare three different couplings  $\Gamma_S = (7.5, 8.0, 8.5)\Gamma_N$  in Fig. 3(a). It is found that the Kondo resonance is significantly enhanced with the increasing coupling  $\Gamma_S$ , which is qualitatively consistent with Domanski *et al.*'s numerical renormalization group calculation.<sup>27</sup>

The constructive role of the superconducting lead on the subgap Kondo transport can also directly checked by comparing the general features of the Kondo transport ( $G_A$ ) for the N-QD-S and ( $G_N$ ) for an N-QD-N devices, as shown in Fig. 4(a) and (b), respectively. For the sake of comparison, we take  $\Gamma_L = \Gamma_N = 0.5\Delta$ . On one hand, the conductance in Fig. 4 (a) is greatly larger than that in Fig. 4 (b), suggesting the constructive effect of the superconducting lead on the Kondo transport, which is in agreement with the experimental observation.<sup>18</sup> On the other hand, although in the both cases the Kondo resonances are obviously underestimated due to the equation of motion method we used, the Kondo peaks in both cases can be suppressed dramatically by increasing temperature. However, up to  $T = 0.04\Delta$ , in the N-QD-N case,

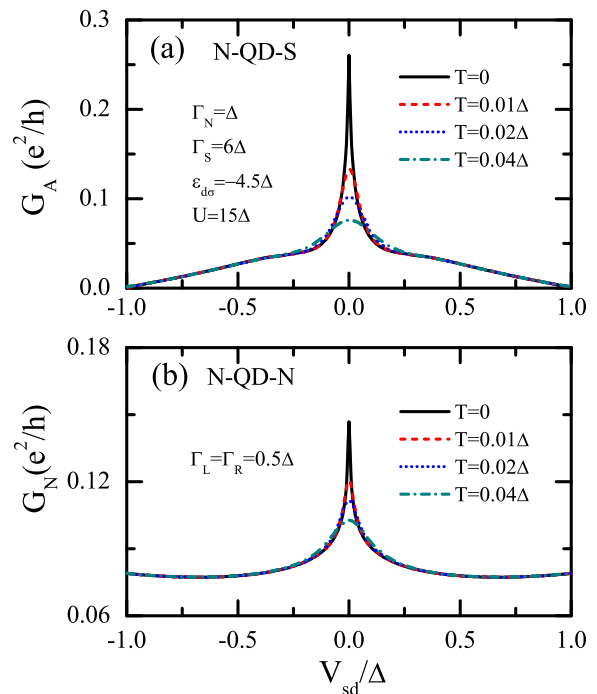


FIG. 4. (a) The temperature dependence of Kondo resonance peak in the Andreev transport of the N-QD-S device. The results are obtained by using the couplings of  $\Gamma_N = \Delta$  and  $\Gamma_S = 6\Delta$ . (b) The temperature dependence of Kondo resonance in a general N-QD-N device by using  $\Gamma_L = \Gamma_R = 0.5\Delta$ . The other parameters used are  $\varepsilon_{d\sigma} = -4.5\Delta$ , and  $U = 15\Delta$ .

a broad peak around the zero bias is still visible, and on the contrary, in the N-QD-S case, the Kondo peak is almost completely killed, which indicates that the Kondo temperature in the N-QD-S should be smaller than that of the N-QD-N. In this sense, our result is also qualitatively compatible with the experimental observation of  $T_K^S \ll T_K^N$ .<sup>18</sup>

#### IV. CONCLUSION

In conclusion, we studied the nature of the Kondo screening in the N-QD-S device. Both the normal and the superconducting leads can contribute to the Kondo effect, but they play different roles in the Kondo screening of local spin. The coupling between the local spin and superconductor induces a pair of Andreev energy levels in the superconducting gap, and it does not directly contribute to the Kondo screening, as the Kondo resonance peak can not be directly observed in the S-QD-S system.<sup>54–58</sup> The ABSs possess effective moment when the ground state of the QD is a magnetic doublet state. When the normal lead is switched on, the Andreev energy levels broaden to form ABSs and at the same time, a Kondo screening happens due to the normal leads. Thus the Kondo resonance in the N-QD-S device can be recognized as the screening of ABSs by the conduction elec-

trons in normal lead. The physical picture can explain qualitatively the experimental observations and may further stimulate the related experimental studies.

Guangdong Province of China 2014A030310137.

### ACKNOWLEDGEMENT

Lin Li acknowledges useful discussion with Hua Chen and Fu-Chun Zhang. This work is supported by NSFC (Grants Nos. 11547110, 11325417, 11204186, 11274269, 11674139) of China, and Natural Science Foundation of

### APPENDIX

In this appendix, we present some main steps to show the truncation approximations in obtaining the Green's functions (GFs) in the main text in the framework of Hartree-Fock (HF) and Lacroix's approximations. The basic starting point is the following equation of motion of the retarded Green's function<sup>59</sup>

$$\omega \langle\langle A; B \rangle\rangle = \langle\langle [A, B]_+ \rangle\rangle + \langle\langle [A, H]_-; B \rangle\rangle, \quad (13)$$

where the subscript  $\pm$  stands for the anti-commutation (commutation) relationship, and  $\langle\langle A; B \rangle\rangle$  denotes the retarded GF composed by the operators  $A$  and  $B$ . From the Hamiltonian Eq.(1) in the main text, one can obtain the GF's of the QD

$$\omega \langle\langle d_\sigma; B \rangle\rangle = \langle\langle [d_\sigma; B]_+ \rangle\rangle + \varepsilon_{d\sigma} \langle\langle d_\sigma; B \rangle\rangle + U \langle\langle d_\sigma n_{d\bar{\sigma}}; B \rangle\rangle + \sum_{k\beta} V_{k\beta}^* \langle\langle c_{k\sigma\beta}; B \rangle\rangle, \quad (14)$$

$$\omega \langle\langle c_{k\sigma\beta}; B \rangle\rangle = \langle\langle [c_{k\sigma\beta}; B]_+ \rangle\rangle + \varepsilon_{k\beta} \langle\langle c_{k\sigma\beta}; B \rangle\rangle + V_{k\beta} \langle\langle d_\sigma; B \rangle\rangle + \sigma \Delta \delta_{\beta,S} \langle\langle c_{-k\bar{\sigma}\beta}^\dagger; B \rangle\rangle, \quad (15)$$

$$\omega \langle\langle c_{-k\bar{\sigma}\beta}^\dagger; B \rangle\rangle = \langle\langle [c_{-k\bar{\sigma}\beta}^\dagger; B]_+ \rangle\rangle - \varepsilon_{-k\beta} \langle\langle c_{-k\bar{\sigma}\beta}^\dagger; B \rangle\rangle - V_{-k\beta}^* \langle\langle d_{\bar{\sigma}}^\dagger; B \rangle\rangle - \bar{\sigma} \Delta^* \delta_{\beta,S} \langle\langle c_{k\sigma\beta}; B \rangle\rangle, \quad (16)$$

$$\omega \langle\langle d_{\bar{\sigma}}^\dagger; B \rangle\rangle = \langle\langle [d_{\bar{\sigma}}^\dagger; B]_+ \rangle\rangle - \varepsilon_{d\bar{\sigma}} \langle\langle d_{\bar{\sigma}}^\dagger; B \rangle\rangle - U \langle\langle d_{\bar{\sigma}}^\dagger n_{d\sigma}; B \rangle\rangle - \sum_{k\beta} V_{-k\beta} \langle\langle c_{-k\bar{\sigma}\beta}^\dagger; B \rangle\rangle, \quad (17)$$

where  $\sigma(\bar{\sigma})$  in the subscript represents the spin orientation  $\uparrow(\downarrow)$  or  $\downarrow(\uparrow)$ , while those appear in the coefficients are set to be  $\pm 1$  for  $\uparrow(\downarrow)$ .

As choosing  $B = d_\sigma^\dagger$  and removing the GFs of  $\langle\langle c_{k\sigma\beta}; B \rangle\rangle$  and  $\langle\langle c_{-k\bar{\sigma}\beta}^\dagger; B \rangle\rangle$  in Eqs.(14)-(17), one can obtain

$$(\omega - \varepsilon_{d\sigma} - \Gamma_1(\omega)) \langle\langle d_\sigma; d_\sigma^\dagger \rangle\rangle + \Delta_1(\omega) \langle\langle d_{\bar{\sigma}}^\dagger; d_\sigma^\dagger \rangle\rangle = 1 + U \langle\langle d_\sigma n_{d\bar{\sigma}}; d_\sigma^\dagger \rangle\rangle, \quad (18)$$

$$(\omega + \varepsilon_{d\bar{\sigma}} - \Gamma_2(\omega)) \langle\langle d_{\bar{\sigma}}^\dagger; d_\sigma^\dagger \rangle\rangle - \Delta_2(\omega) \langle\langle d_\sigma; d_\sigma^\dagger \rangle\rangle = -U \langle\langle d_{\bar{\sigma}}^\dagger n_{d\sigma}; d_\sigma^\dagger \rangle\rangle. \quad (19)$$

Similarly, if one chooses  $B = d_{\bar{\sigma}}$ , we have

$$(\omega - \varepsilon_{d\sigma} - \Gamma_1(\omega)) \langle\langle d_\sigma; d_{\bar{\sigma}} \rangle\rangle + \Delta_1(\omega) \langle\langle d_{\bar{\sigma}}^\dagger; d_{\bar{\sigma}} \rangle\rangle = U \langle\langle d_\sigma n_{d\bar{\sigma}}; d_{\bar{\sigma}} \rangle\rangle, \quad (20)$$

$$(\omega + \varepsilon_{d\bar{\sigma}} - \Gamma_2(\omega)) \langle\langle d_{\bar{\sigma}}^\dagger; d_{\bar{\sigma}} \rangle\rangle - \Delta_2(\omega) \langle\langle d_\sigma; d_{\bar{\sigma}} \rangle\rangle = 1 - U \langle\langle d_{\bar{\sigma}}^\dagger n_{d\sigma}; d_{\bar{\sigma}} \rangle\rangle, \quad (21)$$

where the following notations are introduced for clarity,  $\Gamma_1(\omega) = \sum_{k\beta} \frac{(\omega + \varepsilon_{-k\beta}) V_{k\beta}^* V_{k\beta}}{E_{k\beta}^2}$ ,  $\Gamma_2(\omega) = \sum_{k\beta} \frac{(\omega - \varepsilon_{k\beta}) V_{-k\beta}^* V_{k\beta}}{E_{k\beta}^2}$ ,  $\Delta_1(\omega) = \sum_{k\beta} \frac{\sigma \Delta \delta_{\beta,S} V_{k\beta}^* V_{-k\beta}}{E_{k\beta}^2}$  and  $\Delta_2(\omega) = \sum_{k\beta} \frac{\bar{\sigma} \Delta^* \delta_{\beta,S} V_{k\beta} V_{k\beta}}{E_{k\beta}^2}$  with  $E_{k\beta}^2 = (\omega - \varepsilon_{k\beta})(\omega + \varepsilon_{-k\beta}) - |\Delta|^2 \delta_{\beta,S}$ . To proceed, it is convenient to transform the summation of  $k$  into the integral. For simplicity, in the following it is assumed that the hybrid function is real and  $k$ -independent ( $V_{k\beta} = V_\beta = V_\beta^*$ ), and the superconducting gap is a real constant ( $\Delta = \Delta^*$ ). Then, one obtains  $\Gamma_1(\omega) = \Gamma_2(\omega) = -i\Gamma_N - i\Gamma_{S\rho_S}(\omega) = -i\Gamma(\omega)$  and the notations  $\Delta_1(\omega) = -i\Gamma_{S\rho_S}(\omega) \frac{\sigma\Delta}{\omega}$ ,  $\Delta_2(\omega) = -i\Gamma_{S\rho_S}(\omega) \frac{\bar{\sigma}\Delta}{\omega} = -\Delta_1(\omega)$ , where  $\Gamma_{N/S} = \pi|V_{N/S}|^2 \rho_0$  ( $\rho_0 = 1/2D$ ,  $D$  is the half-bandwidth) and  $\rho_S(\omega) = \frac{|\omega|\theta(|\omega|-\Delta)}{\sqrt{\omega^2-\Delta^2}} + \frac{\omega\theta(\Delta-|\omega|)}{i\sqrt{\Delta^2-\omega^2}}$ .

Introducing the matrix notation

$$\hat{G}_{d\sigma}(\omega) = \begin{pmatrix} \langle\langle d_\sigma; d_\sigma^\dagger \rangle\rangle & \langle\langle d_\sigma; d_{\bar{\sigma}} \rangle\rangle \\ \langle\langle d_{\bar{\sigma}}^\dagger; d_\sigma^\dagger \rangle\rangle & \langle\langle d_{\bar{\sigma}}^\dagger; d_{\bar{\sigma}} \rangle\rangle \end{pmatrix} \quad (22)$$

and

$$\hat{F}_{d\sigma}(\omega) = \begin{pmatrix} \langle\langle d_\sigma n_{d\bar{\sigma}}; d_\sigma^\dagger \rangle\rangle & \langle\langle d_\sigma n_{d\bar{\sigma}}; d_{\bar{\sigma}} \rangle\rangle \\ -\langle\langle d_{\bar{\sigma}}^\dagger n_{d\sigma}; d_\sigma^\dagger \rangle\rangle & -\langle\langle d_{\bar{\sigma}}^\dagger n_{d\sigma}; d_{\bar{\sigma}} \rangle\rangle \end{pmatrix}, \quad (23)$$

the Eqs.(18)-(21) can be rewritten as a matrix form

$$[\hat{G}_{d\sigma}^0(\omega)]^{-1} \hat{G}_{d\sigma}(\omega) = I + U \hat{F}_{d\sigma}(\omega), \quad (24)$$

where  $[\hat{G}_{d\sigma}^0(\omega)]^{-1} = \begin{pmatrix} \omega - \varepsilon_{d\sigma} - \hat{\Sigma}_{11}^0(\omega) & -\hat{\Sigma}_{12}^0(\omega) \\ -\hat{\Sigma}_{21}^0(\omega) & \omega + \varepsilon_{d\bar{\sigma}} - \hat{\Sigma}_{22}^0(\omega) \end{pmatrix}$  and  $\hat{\Sigma}_{11}^0(\omega) = \hat{\Sigma}_{22}^0(\omega) = -i\Gamma(\omega)$ ,  $\hat{\Sigma}_{12}^0(\omega) = \hat{\Sigma}_{21}^0(\omega) = i\Gamma_S\rho_S(\omega)\frac{\sigma\Delta}{\omega}$ . This reproduces the formulas given in Refs.[34] and [35].

It is well-known that Eq.(24) is not closed since  $\hat{F}_{d\sigma}(\omega)$  includes some high-order GFs. To proceed, one needs to employ the truncation approximation. In the following we present some brief steps in deriving the GFs in the HF and the Lacroix's approximate levels.

It is concise to treat  $\hat{F}_{d\sigma}(\omega)$  by the cluster expansion,<sup>36</sup> e.g.,

$$\langle\langle d_\sigma n_{d\bar{\sigma}}; d_\sigma^\dagger \rangle\rangle = \langle n_{d\bar{\sigma}} \rangle \langle\langle d_\sigma; d_\sigma^\dagger \rangle\rangle + \langle d_{\bar{\sigma}} d_\sigma \rangle \langle\langle d_{\bar{\sigma}}^\dagger; d_\sigma^\dagger \rangle\rangle + \langle\langle d_\sigma n_{d\bar{\sigma}}; d_\sigma^\dagger \rangle\rangle_c. \quad (25)$$

One can obtain

$$\hat{F}_{d\sigma}(\omega) = \hat{\Sigma}_{d\sigma}^{HF} \hat{G}_{d\sigma}(\omega) + \hat{F}_{d\sigma}(\omega)_c, \quad (26)$$

where  $\hat{\Sigma}_{d\sigma}^{HF} = \begin{pmatrix} \langle n_{d\bar{\sigma}} \rangle & \langle d_{\bar{\sigma}} d_\sigma \rangle \\ \langle d_\sigma^\dagger d_{\bar{\sigma}}^\dagger \rangle & -\langle n_{d\sigma} \rangle \end{pmatrix}$  represents the non-connected part, while  $\hat{F}_{d\sigma}(\omega)_c = \begin{pmatrix} \langle\langle d_\sigma n_{d\bar{\sigma}}; d_\sigma^\dagger \rangle\rangle_c & \langle\langle d_\sigma n_{d\bar{\sigma}}; d_{\bar{\sigma}} \rangle\rangle_c \\ -\langle\langle d_{\bar{\sigma}}^\dagger n_{d\sigma}; d_\sigma^\dagger \rangle\rangle_c & -\langle\langle d_{\bar{\sigma}}^\dagger n_{d\sigma}; d_{\bar{\sigma}} \rangle\rangle_c \end{pmatrix}$  denotes connected (residual) part. In Eq.(24),  $U\hat{F}_{d\sigma}(\omega)$  corresponds to the HF self-energy if  $\hat{F}_{d\sigma}(\omega)_c$  is neglected,<sup>33,38,39</sup> and one has

$$\left([\hat{G}_{d\sigma}^0(\omega)]^{-1} - U\hat{\Sigma}_{d\sigma}^{HF}\right) \hat{G}_{d\sigma}(\omega) = I. \quad (27)$$

Beyond the HF approximation, one needs to take  $\hat{F}_{d\sigma}(\omega)_c$  into account, which is a bit complex but straightforward. Here our main aim is to study the interplay between the superconductivity and the Kondo effect. While superconductivity is already available in the superconducting lead, the diagonal components in  $\hat{F}_{d\sigma}(\omega)_c$  is sufficient to capture the Kondo effect in the Lacroix's approximation level. Therefore, in the following we neglect anomalous high-order GFs like  $\langle\langle d_\sigma n_{d\bar{\sigma}}; d_{\bar{\sigma}} \rangle\rangle_c$  and  $\langle\langle d_{\bar{\sigma}}^\dagger n_{d\sigma}; d_\sigma^\dagger \rangle\rangle_c$  for simplification. Immediately, one can obtain

$$\langle\langle d_{\bar{\sigma}}^\dagger; d_\sigma^\dagger \rangle\rangle = \frac{\hat{\Sigma}_{21}^0(\omega) + U\langle d_\sigma^\dagger d_{\bar{\sigma}}^\dagger \rangle}{\omega + \varepsilon_{d\bar{\sigma}} - \hat{\Sigma}_{22}^0(\omega) + U\langle n_{d\sigma} \rangle} \langle\langle d_\sigma; d_\sigma^\dagger \rangle\rangle, \quad (28)$$

and

$$\left(\omega - \varepsilon_{d\sigma} - \hat{\Sigma}_{11}^0(\omega) - U\langle n_{d\bar{\sigma}} \rangle\right) \langle\langle d_\sigma; d_\sigma^\dagger \rangle\rangle - \left(\hat{\Sigma}_{12}^0(\omega) + U\langle d_{\bar{\sigma}} d_\sigma \rangle\right) \langle\langle d_{\bar{\sigma}}^\dagger; d_\sigma^\dagger \rangle\rangle = 1 + \langle\langle d_\sigma n_{d\bar{\sigma}}; d_\sigma^\dagger \rangle\rangle_c. \quad (29)$$

Above equations can be calculated self-consistently if we obtain  $\langle\langle d_\sigma n_{d\bar{\sigma}}; d_\sigma^\dagger \rangle\rangle_c$ . For  $\langle\langle d_\sigma; d_{\bar{\sigma}} \rangle\rangle$  and  $\langle\langle d_{\bar{\sigma}}^\dagger; d_{\bar{\sigma}} \rangle\rangle$  one has a similar treatment (not shown here) for clarity.

To obtain the equation of motion of  $\langle\langle d_\sigma n_{d\bar{\sigma}}; d_\sigma^\dagger \rangle\rangle_c$ , we start from the equation of motion of the Green's function  $\langle\langle d_\sigma n_{d\bar{\sigma}}; d_\sigma^\dagger \rangle\rangle$ ,

$$(\omega - \varepsilon_{d\sigma} - U)\langle\langle d_\sigma n_{d\bar{\sigma}}; d_\sigma^\dagger \rangle\rangle = \langle n_{d\bar{\sigma}} \rangle + \sum_{k\beta} V_\beta \langle\langle c_{k\sigma\beta} n_{d\bar{\sigma}}; d_\sigma^\dagger \rangle\rangle + \sum_{k\beta} V_\beta \left( \langle\langle d_{\bar{\sigma}}^\dagger c_{-k\bar{\sigma}\beta} d_\sigma; d_\sigma^\dagger \rangle\rangle - \langle\langle c_{-k\bar{\sigma}\beta}^\dagger d_{\bar{\sigma}} d_\sigma; d_\sigma^\dagger \rangle\rangle \right), \quad (30)$$

which involves other high-order GFs  $\langle\langle c_{k\sigma\beta} n_{d\bar{\sigma}}; d_\sigma^\dagger \rangle\rangle$ ,  $\langle\langle d_{\bar{\sigma}}^\dagger c_{-k\bar{\sigma}\beta} d_\sigma; d_\sigma^\dagger \rangle\rangle$ , and  $\langle\langle c_{-k\bar{\sigma}\beta}^\dagger d_{\bar{\sigma}} d_\sigma; d_\sigma^\dagger \rangle\rangle$ , whose equations of motion are given as follows

$$\begin{aligned} (\omega - \varepsilon_{k\beta})\langle\langle c_{k\sigma\beta} n_{d\bar{\sigma}}; d_\sigma^\dagger \rangle\rangle &= V_\beta \langle\langle d_\sigma n_{d\bar{\sigma}}; d_\sigma^\dagger \rangle\rangle + \sigma\Delta\delta_{\beta,S} \langle\langle c_{-k\bar{\sigma}\beta}^\dagger n_{d\bar{\sigma}}; d_\sigma^\dagger \rangle\rangle \\ &+ \sum_{k'\beta'} V_{\beta'} \langle\langle d_{\bar{\sigma}}^\dagger c_{-k'\bar{\sigma}\beta'} c_{k\sigma\beta}; d_\sigma^\dagger \rangle\rangle - \sum_{k'\beta'} V_{\beta'} \langle\langle c_{-k'\bar{\sigma}\beta'}^\dagger d_{\bar{\sigma}} c_{k\sigma\beta}; d_\sigma^\dagger \rangle\rangle, \end{aligned} \quad (31)$$

$$\begin{aligned} (\omega - \omega_{1,k\sigma\beta})\langle\langle d_{\bar{\sigma}}^\dagger c_{-k\bar{\sigma}\beta} d_\sigma; d_\sigma^\dagger \rangle\rangle &= \langle d_{\bar{\sigma}}^\dagger c_{-k\bar{\sigma}\beta} \rangle + V_\beta \langle\langle d_\sigma n_{\bar{\sigma}}; d_\sigma^\dagger \rangle\rangle - \sum_{k'\beta'} V_{\beta'} \langle\langle c_{-k'\bar{\sigma}\beta'}^\dagger c_{-k\bar{\sigma}\beta} d_\sigma; d_\sigma^\dagger \rangle\rangle \\ &+ \sum_{k'\beta'} V_{\beta'} \langle\langle d_{\bar{\sigma}}^\dagger c_{-k\bar{\sigma}\beta} c_{k'\sigma\beta'}; d_\sigma^\dagger \rangle\rangle + \bar{\sigma}\Delta\delta_{\beta,S} \langle\langle d_{\bar{\sigma}}^\dagger c_{k\sigma\beta}^\dagger d_\sigma; d_\sigma^\dagger \rangle\rangle, \end{aligned} \quad (32)$$

$$\begin{aligned}
(\omega - \omega_{2,k\sigma\beta}) \langle \langle c_{-k\bar{\sigma}\beta}^\dagger d_{\bar{\sigma}} d_{\sigma}; d_{\sigma}^\dagger \rangle \rangle &= \langle c_{-k\bar{\sigma}\beta}^\dagger d_{\bar{\sigma}} \rangle - V_{\beta} \langle \langle d_{\sigma} n_{\bar{\sigma}}; d_{\sigma}^\dagger \rangle \rangle - \bar{\sigma} \Delta \delta_{\beta,S} \langle \langle c_{k\sigma\beta} d_{\bar{\sigma}} d_{\sigma}; d_{\sigma}^\dagger \rangle \rangle \\
&+ \sum_{k'\beta'} V_{\beta'} \langle \langle c_{-k\bar{\sigma}\beta}^\dagger c_{-k'\bar{\sigma}\beta'} d_{\sigma}; d_{\sigma}^\dagger \rangle \rangle + \sum_{k'\beta'} V_{\beta'} \langle \langle c_{-k\bar{\sigma}\beta}^\dagger d_{\bar{\sigma}} c_{k'\sigma\beta'}; d_{\sigma}^\dagger \rangle \rangle, \quad (33)
\end{aligned}$$

where  $\omega_{1,k\sigma\beta} = \varepsilon_{-k\beta} + \varepsilon_{d\sigma} - \varepsilon_{d\bar{\sigma}}$  and  $\omega_{2,k\sigma\beta} = -\varepsilon_{-k\beta} + \varepsilon_{d\bar{\sigma}} + \varepsilon_{d\sigma} + U$ . In order to obtain  $\langle \langle d_{\sigma} n_{d\bar{\sigma}}; d_{\sigma}^\dagger \rangle \rangle_c$ , the other high-order GFs involved in Eqs.(31)-(33) have been treated by the cluster expansion, e.g.,  $\langle \langle c_{k\sigma\beta} n_{d\bar{\sigma}}; d_{\sigma}^\dagger \rangle \rangle \approx \langle n_{d\bar{\sigma}} \rangle \langle \langle c_{k\sigma\beta}; d_{\sigma}^\dagger \rangle \rangle + \langle \langle c_{k\sigma\beta} n_{d\bar{\sigma}}; d_{\sigma}^\dagger \rangle \rangle_c$ . Here, the additional approximation taken is to neglect all superconducting correlation functions involved QD-leads pairing. For the same reason, the possible pairing corrections brought from the higher order GFs like  $\langle \langle c_{-k\bar{\sigma}\beta}^\dagger n_{d\bar{\sigma}}; d_{\sigma}^\dagger \rangle \rangle$ ,  $\langle \langle d_{\bar{\sigma}}^\dagger c_{-k\sigma\beta}^\dagger d_{\sigma}; d_{\sigma}^\dagger \rangle \rangle$  and  $\langle \langle c_{-k\sigma\beta} d_{\bar{\sigma}} d_{\sigma}; d_{\sigma}^\dagger \rangle \rangle$  are also neglected.

After a long but straightforward calculation, one has

$$\begin{aligned}
(\omega - \varepsilon_{d\sigma} - U(1 - \langle n_{d\bar{\sigma}} \rangle)) \langle \langle d_{\sigma} n_{d\bar{\sigma}}; d_{\sigma}^\dagger \rangle \rangle_c &= U[\langle n_{d\bar{\sigma}} \rangle (1 - \langle n_{d\bar{\sigma}} \rangle) - \langle d_{\bar{\sigma}} d_{\sigma} \rangle \langle d_{\sigma}^\dagger d_{\bar{\sigma}}^\dagger \rangle] \langle \langle d_{\sigma}; d_{\sigma}^\dagger \rangle \rangle \\
&+ [\varepsilon_{d\sigma} + \varepsilon_{d\bar{\sigma}} + U(1 - \langle n_{d\bar{\sigma}} \rangle + \langle n_{d\sigma} \rangle)] \langle d_{\bar{\sigma}} d_{\sigma} \rangle \langle \langle d_{\bar{\sigma}}^\dagger; d_{\sigma}^\dagger \rangle \rangle + \sum_{k\beta} V_{\beta} \langle \langle c_{k\sigma\beta} n_{d\bar{\sigma}}; d_{\sigma}^\dagger \rangle \rangle_c \\
&- \sum_{k\beta} V_{\beta} \langle \langle c_{-k\bar{\sigma}\beta}^\dagger d_{\bar{\sigma}} d_{\sigma}; d_{\sigma}^\dagger \rangle \rangle_c + \sum_{k\beta} V_{\beta} \langle \langle d_{\bar{\sigma}}^\dagger c_{-k\bar{\sigma}\beta} d_{\sigma}; d_{\sigma}^\dagger \rangle \rangle_c, \quad (34)
\end{aligned}$$

Likewise, the more higher order connected GFs read

$$(\omega - \varepsilon_{k\beta}) \langle \langle c_{k\sigma\beta} n_{d\bar{\sigma}}; d_{\sigma}^\dagger \rangle \rangle_c \approx V_{\beta} \langle \langle d_{\sigma} n_{d\bar{\sigma}}; d_{\sigma}^\dagger \rangle \rangle_c, \quad (35)$$

$$(\omega - \omega_{1,k\sigma\beta}) \langle \langle d_{\bar{\sigma}}^\dagger c_{-k\bar{\sigma}\beta} d_{\sigma}; d_{\sigma}^\dagger \rangle \rangle_c \approx A_{1,k\sigma\beta} \langle \langle d_{\sigma}; d_{\sigma}^\dagger \rangle \rangle + B_{1,k\sigma\beta} \langle \langle d_{\sigma} n_{d\bar{\sigma}}; d_{\sigma}^\dagger \rangle \rangle_c, \quad (36)$$

$$(\omega - \omega_{2,k\sigma\beta}) \langle \langle c_{-k\bar{\sigma}\beta}^\dagger d_{\bar{\sigma}} d_{\sigma}; d_{\sigma}^\dagger \rangle \rangle_c \approx A_{2,k\sigma\beta} \langle \langle d_{\sigma}; d_{\sigma}^\dagger \rangle \rangle - B_{2,k\sigma\beta} \langle \langle d_{\sigma} n_{d\bar{\sigma}}; d_{\sigma}^\dagger \rangle \rangle_c, \quad (37)$$

where

$$A_{1,k\sigma\beta} = (\omega_{1,k\sigma\beta} - \varepsilon_{d\sigma} - U \langle n_{d\bar{\sigma}} \rangle) \langle d_{\bar{\sigma}}^\dagger c_{-k\bar{\sigma}\beta} \rangle + V_{\beta} \langle n_{d\bar{\sigma}} \rangle - \sum_{k'\beta'} V_{\beta'} \langle c_{-k'\bar{\sigma}\beta'}^\dagger c_{-k\bar{\sigma}\beta} \rangle, \quad (38)$$

$$A_{2,k\sigma\beta} = (\omega_{2,k\sigma\beta} - \varepsilon_{d\sigma} - U \langle n_{d\bar{\sigma}} \rangle) \langle c_{-k\bar{\sigma}\beta}^\dagger d_{\bar{\sigma}} \rangle - V_{\beta} \langle n_{d\bar{\sigma}} \rangle + \sum_{k'\beta'} V_{\beta'} \langle c_{-k'\bar{\sigma}\beta'}^\dagger c_{-k\bar{\sigma}\beta} \rangle, \quad (39)$$

and  $B_{1,k\sigma\beta} = V_{\beta} - U \langle d_{\bar{\sigma}}^\dagger c_{-k\bar{\sigma}\beta} \rangle$ ,  $B_{2,k\sigma\beta} = V_{\beta} + U \langle c_{-k\bar{\sigma}\beta}^\dagger d_{\bar{\sigma}} \rangle$ . The truncation scheme taken above in the derivation of Eqs. (34)-(37) is essentially the famous Lacroix's approximation, which is sufficient to capture qualitatively the Kondo effect.<sup>36,40</sup>

By substituting Eqs.(35)-(37) into Eq.(34), then going back to Eq.(29), in combination with Eq.(28), one has

$$\langle \langle d_{\sigma}; d_{\sigma}^\dagger \rangle \rangle = \frac{1}{R_{\sigma}(\omega) - U[Q_{\sigma}(\omega) + T_{\sigma}(\omega)]/P_{\sigma}(\omega)}, \quad (40)$$

where

$$R_{\sigma}(\omega) = \omega - \varepsilon_{d\sigma} + i\Gamma(\omega) - U \langle n_{d\bar{\sigma}} \rangle - \frac{(\hat{\Sigma}_{21}^0(\omega) + U \langle d_{\bar{\sigma}} d_{\sigma} \rangle)(\hat{\Sigma}_{21}^0(\omega) + U \langle d_{\sigma}^\dagger d_{\bar{\sigma}}^\dagger \rangle)}{\omega + \varepsilon_{d\bar{\sigma}} + i\Gamma(\omega) + U \langle n_{d\sigma} \rangle}, \quad (41)$$

$$P_{\sigma}(\omega) = \omega - \varepsilon_{d\sigma} - U(1 - \langle n_{d\bar{\sigma}} \rangle) + 3i\Gamma(\omega) + U(A_{1\sigma}(\omega) - A_{2\sigma}(\omega)), \quad (42)$$

$$\begin{aligned}
Q_{\sigma}(\omega) &= (\omega - \varepsilon_{d\sigma} - U \langle n_{d\bar{\sigma}} \rangle) (A_{1\sigma}(\omega) - A_{2\sigma}(\omega)) + U[\langle n_{d\bar{\sigma}} \rangle (1 - \langle n_{d\bar{\sigma}} \rangle) - \langle d_{\bar{\sigma}} d_{\sigma} \rangle \langle d_{\sigma}^\dagger d_{\bar{\sigma}}^\dagger \rangle] \\
&- 2i\Gamma(\omega) \langle n_{d\bar{\sigma}} \rangle - (B_{1\sigma}(\omega) + B_{2\sigma}(\omega)), \quad (43)
\end{aligned}$$

$$T_{\sigma}(\omega) = [\varepsilon_{d\sigma} + \varepsilon_{d\bar{\sigma}} + U(1 + \langle n_{d\sigma} \rangle - \langle n_{d\bar{\sigma}} \rangle)] \frac{\langle d_{\bar{\sigma}} d_{\sigma} \rangle (\hat{\Sigma}_{21}^0(\omega) + U \langle d_{\sigma}^\dagger d_{\bar{\sigma}}^\dagger \rangle)}{\omega + \varepsilon_{d\bar{\sigma}} + i\Gamma(\omega) + U \langle n_{d\sigma} \rangle}. \quad (44)$$

In  $P_{\sigma}(\omega)$  and  $Q_{\sigma}(\omega)$ , the notation

$$\begin{aligned}
A_{i\sigma}(\omega) &= \sum_{k\beta} \frac{V_{\beta} \langle d_{\bar{\sigma}}^\dagger c_{-k\bar{\sigma}\beta} \rangle}{z_+ - \omega_{i,k\sigma\beta}} \\
&= \frac{i}{2\pi} \sum_{k\beta} \frac{1}{z_+ - \omega_{i,k\sigma\beta}} \int d\omega' f(\omega') V_{\beta} (\langle \langle c_{-k\bar{\sigma}\beta}; d_{\bar{\sigma}}^\dagger \rangle \rangle_{\omega'}^r - \langle \langle c_{-k\bar{\sigma}\beta}; d_{\bar{\sigma}}^\dagger \rangle \rangle_{\omega'}^a) \\
&= \frac{i}{2\pi^2} \sum_{\beta} \int \int d\omega' d\varepsilon \Gamma_{\beta} f(\omega') \frac{\frac{(z_+ + \varepsilon) \langle \langle d_{\bar{\sigma}}; d_{\bar{\sigma}}^\dagger \rangle \rangle_{\omega'}^r - \delta_{\beta,S} \bar{\sigma} \Delta \langle \langle d_{\sigma}^\dagger; d_{\bar{\sigma}}^\dagger \rangle \rangle_{\omega'}^r}{(z_+ - \varepsilon)(z_+ + \varepsilon) - \delta_{\beta,S} \Delta^2} - \frac{(z_+ + \varepsilon) \langle \langle d_{\bar{\sigma}}; d_{\bar{\sigma}}^\dagger \rangle \rangle_{\omega'}^a - \delta_{\beta,S} \bar{\sigma} \Delta \langle \langle d_{\sigma}^\dagger; d_{\bar{\sigma}}^\dagger \rangle \rangle_{\omega'}^a}{(z_+ - \varepsilon)(z_+ + \varepsilon) - \delta_{\beta,S} \Delta^2}}{z_+ - \varepsilon_{i\sigma}}
\end{aligned} \quad (45)$$

where  $z_{\pm} = \omega \pm i0^+$ ,  $\varepsilon_{1\sigma} = \varepsilon + \varepsilon_{d\sigma} - \varepsilon_{d\bar{\sigma}}$ , and  $\varepsilon_{2\sigma} = -\varepsilon + \varepsilon_{d\bar{\sigma}} + \varepsilon_{d\sigma} + U$ . The average value  $\langle d_{\bar{\sigma}}^{\dagger} c_{-k\bar{\sigma}\beta} \rangle$  is calculated by the spectral theorem  $\langle d_{\bar{\sigma}}^{\dagger} c_{-k\bar{\sigma}\beta} \rangle = \frac{i}{2\pi} \int d\omega f(\omega) (\langle \langle c_{-k\bar{\sigma}\beta}; d_{\bar{\sigma}}^{\dagger} \rangle_{\omega}^r - \langle \langle c_{-k\bar{\sigma}\beta}; d_{\bar{\sigma}}^{\dagger} \rangle_{\omega}^a)$ , and  $\langle c_{-k\bar{\sigma}\beta}^{\dagger} d_{\bar{\sigma}} \rangle = \langle d_{\bar{\sigma}}^{\dagger} c_{-k\bar{\sigma}\beta} \rangle$  is taken in Eq.(42) and Eq.(43). The GF obtained is  $\langle \langle c_{k\bar{\sigma}\beta}; d_{\bar{\sigma}}^{\dagger} \rangle_{\omega}^{r(a)} = \frac{(z_{\pm} + \varepsilon_{-k\beta}) V_{\beta} \langle \langle d_{\bar{\sigma}}; d_{\bar{\sigma}}^{\dagger} \rangle_{\omega}^{r(a)} - \delta_{\beta,S} \bar{\sigma} \Delta V_{\beta} \langle \langle d_{\bar{\sigma}}^{\dagger}; d_{\bar{\sigma}} \rangle_{\omega}^{r(a)} \rangle}{(z_{\pm} - \varepsilon_{k\beta})(z_{\pm} + \varepsilon_{-k\beta}) - \delta_{\beta,S} \Delta^2}$ . Similarly, we can obtain

$$\begin{aligned} B_{i\sigma}(\omega) &= \sum_{kk'\beta\beta'} \frac{|V_{\beta}|^2 \langle c_{-k'\bar{\sigma}\beta'}^{\dagger} c_{-k\bar{\sigma}\beta} \rangle}{z_{+} - \omega_{i,k\sigma\beta}} \\ &= \frac{i}{2\pi} \sum_{kk'\beta\beta'} \int d\omega' f(\omega') \frac{V_{\beta} V_{\beta'} (\langle \langle c_{-k\bar{\sigma}\beta}; c_{-k'\bar{\sigma}\beta'}^{\dagger} \rangle_{\omega'}^r - \langle \langle c_{-k\bar{\sigma}\beta}; c_{-k'\bar{\sigma}\beta'}^{\dagger} \rangle_{\omega'}^a)}{z_{+} - \omega_{i,k\sigma\beta}} \\ &\approx \frac{1}{\pi} \int d\varepsilon \frac{\Gamma_N f(\varepsilon) (1 - i\Gamma_N \langle \langle d_{\bar{\sigma}}; d_{\bar{\sigma}}^{\dagger} \rangle_{\varepsilon}^r)}{z_{+} - \varepsilon_{i\sigma}} + \frac{i}{2\pi^2} \int \int d\omega' d\varepsilon f(\omega') \Gamma_S(\varepsilon) \frac{\frac{z'_{+} + \varepsilon}{(z'_{+} - \varepsilon)(z'_{+} + \varepsilon) - \Delta^2} - \frac{z'_{-} + \varepsilon}{(z'_{-} - \varepsilon)(z'_{-} + \varepsilon) - \Delta^2}}{z_{+} - \varepsilon_{i\sigma}}, \end{aligned} \quad (46)$$

where  $\langle c_{-k'\bar{\sigma}\beta'}^{\dagger} c_{-k\bar{\sigma}\beta} \rangle = \frac{i}{2\pi} \int d\omega f(\omega) (\langle \langle c_{-k\bar{\sigma}\beta}; c_{-k'\bar{\sigma}\beta'}^{\dagger} \rangle_{\omega}^r - \langle \langle c_{-k\bar{\sigma}\beta}; c_{-k'\bar{\sigma}\beta'}^{\dagger} \rangle_{\omega}^a)$ , and the GFs involved can be approximately obtained with  $\sum_{\beta\beta'=(N,S)} \langle \langle c_{k\bar{\sigma}\beta}; c_{k'\bar{\sigma}\beta'}^{\dagger} \rangle_{\omega}^{r(a)} \approx \frac{\delta_{kk'}}{z_{\pm} - \varepsilon_{kN}} + \frac{|V_N|^2 \langle \langle d_{\bar{\sigma}}; d_{\bar{\sigma}}^{\dagger} \rangle_{\omega}^{r(a)} \rangle}{(z_{\pm} - \varepsilon_{kN})(z_{\pm} - \varepsilon_{k'N})} + \frac{(z'_{\pm} + \varepsilon_{kS}) \delta_{kk'}}{(z'_{\pm} - \varepsilon_{kS})(z'_{\pm} + \varepsilon_{-kS}) - \Delta^2}$ .

- 
- <sup>1</sup> J. Kondo, Prog. Theor. Phys. **32**, 37 (1964).
  - <sup>2</sup> L. Yu, Acta Phys. Sin. **21**, 75 (1965).
  - <sup>3</sup> H. Shiba, Prog. Theor. Phys. **40**, 435 (1968).
  - <sup>4</sup> A. I. Rusinov, Zh. Eksp. Teor. Fiz. **56**, 2047 (1969) [Sov. Phys. JETP **29**, 1101 (1969)].
  - <sup>5</sup> M. E. Flatté and J. M. Byers, Phys. Rev. Lett. **78**, 3761 (1997).
  - <sup>6</sup> K. J. Franke, G. Schulze, and J. I. Pascual, Science **332**, 940 (2011).
  - <sup>7</sup> C. W. J. Beenakker *Transport Phenomena in Mesoscopic Systems* (eds H. Fukuyama and T. Ando) (Springer, 1992).
  - <sup>8</sup> A. Zazunov, V. S. Shumeiko, E. N. Bratus', J. Lantz, and G. Wendin, Phys. Rev. Lett. **90**, 087003 (2003).
  - <sup>9</sup> Y. Avishai, A. Golub, and A. D. Zaikin, Phys. Rev. B **63**, 134515 (2001); Phys. Rev. B **67**, 041301(R) (2003).
  - <sup>10</sup> A. Ossipov, M. Titov, C. W. J. Beenakker, Phys. Rev. B **75**, 241401 (2007).
  - <sup>11</sup> Z. Y. Zhang, J. Phys. Condens. Matter **20**, 443220 (2008).
  - <sup>12</sup> J. Skoldberg, T. Lofwander, V. S. Shumeiko, and M. Fogelström, Phys. Rev. Lett. **101**, 087002 (2008).
  - <sup>13</sup> T. Meng, S. Florens and P. Simon, Phys. Rev. B **79**, 224521 (2009).
  - <sup>14</sup> R. S. Deacon, Y. Tanaka, A. Oiwa, R. Sakano, K. Yoshida, K. Shibata, K. Hirakawa, and S. Tarucha, Phys. Rev. Lett. **104**, 076805 (2010).
  - <sup>15</sup> W. Chang, V. E. Manucharyan, T. S. Jespersen, J. Nygard, and C. M. Marcus, Phys. Rev. Lett. **110**, 217005 (2013).
  - <sup>16</sup> E. J. H. Lee, X. C. Jia, M. Houzet, R. Aguado, C. M. Lieber, and S. D. Franceschi, Nature Nanotechnol. **9**, 79-84 (2014).
  - <sup>17</sup> T. Dirks *et al.*, Nat. Phys. **7**, 386 (2011).
  - <sup>18</sup> R. S. Deacon, Y. Tanaka, A. Oiwa, R. Sakano, K. Yoshida, K. Shibata, K. Hirakawa, and S. Tarucha, Phys. Rev. B **81**, 121308(R) (2010).
  - <sup>19</sup> A. A. Clerk, V. Ambegaokar, and S. Hershfield, Phys. Rev. B **61**, 3555 (2000).
  - <sup>20</sup> Q. -F. Sun, H. Guo, and T. -H. Lin, Phys. Rev. Lett. **87**, 176601 (2001).
  - <sup>21</sup> M. Krawiec and K. I. Wysokiński, Supercond. Sci. Technol. **17**, 103 (2004).
  - <sup>22</sup> A. Golub, and Y. Avishai, Phys. Rev. B **69**, 165325 (2004).
  - <sup>23</sup> T. Domanski and A. Donabidowicz, Phys. Rev. B **78**, 073105 (2008).
  - <sup>24</sup> V. Koerting, B. M. Andersen, K. Flensberg, and J. Paaske, Phys. Rev. B **82**, 245108 (2010).
  - <sup>25</sup> Y. Yamada, Y. Tanaka, and N. Kawakami, Phys. Rev. B **84**, 075484 (2011).
  - <sup>26</sup> R. Zitko, J. S. Lim, R. Lopez, and R. Aguado, Phys. Rev. B **91**, 045441 (2015).
  - <sup>27</sup> T. Domanski, I. Weymann, M. Baranska, and G. Gorski, arXiv:1507.01851 (2015).
  - <sup>28</sup> P. W. Anderson, Phys. Rev. **124**, 41 (1961).
  - <sup>29</sup> Q-F Sun, J. Wang, and T-H Lin, Phys. Rev. B **62**, 648 (2000).
  - <sup>30</sup> Y. Tanaka, N. Kawakami, and A. Oguri, J. Phys. Soc. Jpn. **76** 074701 (2007).
  - <sup>31</sup> T. Domański, A. Donabidowicz, and K. I. Wysokiński, Phys. Rev. B **78**, 144515 (2008).
  - <sup>32</sup> J. Barański and T. Domański, Phys. Rev. B **84**, 195424 (2011).
  - <sup>33</sup> E. Vecino, A. Martín-Rodero, and A. Levy Yeyati, Phys. Rev. B **68**, 035105 (2003).
  - <sup>34</sup> J. Bauer, A. Oguri, and A. C. Hewson, J. Phys.: Condens. Matter **19**, 486211 (2007).
  - <sup>35</sup> R. Bulla, A. C. Hewson, and T. Pruschke, J. Phys.: Condens. Matter **10**, 8365 (1998).
  - <sup>36</sup> H.-G. Luo, Z.-J. Ying, and S.-J. Wang, Phys. Rev. B **59**, 9710 (1999).
  - <sup>37</sup> K. Osawa, S. Kurihara, and N. Yokoshi, Phys. Rev. B **78**, 224508 (2008).
  - <sup>38</sup> J. C. Cuevas, A. Levy Yeyati, and A. Martin-Rodero, Phys. Rev. B **63**, 094515 (2001).

- <sup>39</sup> C. Benjamin, T. Jonckheere, A. Zazunov, and T. Martin, *Eur. Phys. J. B* **57**, 279 (2007).
- <sup>40</sup> C. Lacroix, *J. Phys. F* **11**, 2389 (1981).
- <sup>41</sup> J. Barański and T. Domański, *J. Phys.:Condens. Matter* **25** 435305 (2013).
- <sup>42</sup> S.-y. Shiau, S. Chutia, and R. Joynt, *Phys. Rev. B* **75**, 195345 (2007).
- <sup>43</sup> Y. Qi, J.-X. Zhu, S. Zhang, and C. S. Ting, *Phys. Rev. B* **78**, 045305 (2008).
- <sup>44</sup> Q. Feng, Y.-Z. Zhang, and H. O. Jeschke, *Phys. Rev. B* **79**, 235112 (2009).
- <sup>45</sup> T.-F. Fang, W. Zuo, and H.-G. Luo, *Phys. Rev. Lett.* **101**, 246805 (2008); **104**, 169902(E) (2010).
- <sup>46</sup> J. S. Lim, R. López, L. Limot, and P. Simon, *Phys. Rev. B* **88**, 165403 (2013).
- <sup>47</sup> D. Krychowski, J. Kaczkowski, and S. Lipinski, *Phys. Rev. B* **89**, 035424 (2014).
- <sup>48</sup> L. Li, B.-B. Zheng, W.-Q. Chen, H. Chen, H.-G. Luo, and F.-C. Zhang, *Phys. Rev. B* **89**, 245135 (2014).
- <sup>49</sup> G. Sellier, T. Kopp, J. Kroha, and Y. S. Barash, *Phys. Rev. B* **72**, 174502 (2005).
- <sup>50</sup> L. Li, Z. Cao, H.-G. Luo, F.-C. Zhang, W.-Q. Chen, *Phys. Rev. B* **92**, 195155 (2015).
- <sup>51</sup> T. A. Costi, A. C. Hewson, and V. Zlati, *J. Phys. Condens. Matter* **6**, 2519 (1994).
- <sup>52</sup> H.-G. Luo, T. Xiang, X.-Q. Wang, Z.-B. Su, and L. Yu, *Phys. Rev. Lett.* **92**, 256602 (2004).
- <sup>53</sup> T.-F. Fang, N.-H. Tong, Z. Cao, Q.-F. Sun, and H.-G. Luo, *Phys. Rev. B* **92**, 155129 (2015).
- <sup>54</sup> S. De Franceschi, L. Kouwenhoven, C. Schönenberger, and W. Wernsdorfer, *Nature Nanotechnology* **5**, 703 (2010).
- <sup>55</sup> R. Maurand, T. Meng, E. Bonet, S. Florens, L. Marty, and W. Wernsdorfer, *Phys. Rev. X* **2**, 011009 (2012).
- <sup>56</sup> J.-D. Pillet, P. Joyez, R. Zitko, and M. F. Goffman, *Phys. Rev. B* **88**, 045101 (2013).
- <sup>57</sup> B.-K. Kim, Y.-H. Ahn, J.-J. Kim, M.-S Choi, M.-H. Bae, K. Kang, J. S. Lim, R. López, and N. Kim, *Phys. Rev. Lett.* **110**, 076803 (2013).
- <sup>58</sup> A. Kumar, M. Gaim, D. Steininger, A. Levy Yeyati, A. Martin-Rodero, A. K. Hüttel, and C. Strunk, *Phys. Rev. B* **89**, 075428 (2014).
- <sup>59</sup> D. N. Zubarev, *Usp. Fiz. Nauk* **71**, 71 (1960) [*Sov. Phys. Usp.* **3**, 320 (1960)].